Transactions of the Materials Research Society of Japan 29 [2] 409-412 (2004)

Design of Thin Films with Tailored Nano-morphology

Motofumi Suzuki[a], Kenji Kimura[a] and Yasunori Taga[b]
[a]Department of Engineering Physics and Mechanics, Kyoto University, Kyoto 606-8501, Japan
Fax: 81-75-753-5196, e-mail: m-snki@kues.kyoto-u.ac.jp
[b]TOYOTA Central R & D Labs., Inc., Nagakute, Aichi 480-1192, Japan

In order to design thin films prepared by dynamic oblique deposition, we have calibrated the parameters of the fully 3-dimensional thin film growth simulator VFIGS (Virtual Film Growth System). Using the parameters calibrated for Si, we have simulated the density modulated thin films which are deposited by varying the deposition angle α sinusoidally. When the maximum α exceeds 85°, significant columnar broadening has occurred, and the amplitude of the density oscillation has been degraded. On the other hand, the amplitude and the period of density are kept constant when the maximum α is less than 85°. The density can be controlled arbitrarily between 0.45 and 0.86 which correspond to the refractive index of 1.6 and 2.8 for Si.
Key words: oblique deposition, nanostructure, columnar structure, thin film growth

1. INTRODUCTION

Unique structures and properties of obliquely deposited thin films have been extensively investigated since the end of the 1950s, while the history of the studies of obliquely deposited thin films is more than a century [1]. The physical origins of the columnar structure in obliquely deposited thin films are the self-shadowing effects and the limited mobility of the deposited atoms [2]. When the vapor flux is obliquely incident, atoms in the growing films shadow unoccupied sites from the direct sticking of incident atoms. Moreover, owing to limited mobility, the unoccupied sites are not filled later. As a result, oblique columns grow in the direction of the incident vapor beam.

In 1989, Motohiro and Taga [3] successfully developed inorganic thin-film waveplates with a chevron-shaped columnar structure using bidirectional oblique deposition. Subsequently, we applied the obliquely deposited Ta_2O_5 thin films to the waveplate for optical pickups [4]. Recently, thin films with highly controlled isolated columns such as helix [5] and zigzag [6] have been developed. Furthermore, integration of these morphologies has been achieved [7]. These 'hypercolumnar' structures are engineered by dynamic oblique deposition (DOD), in which the deposition angle and/or the azimuthal deposition direction are varied dynamically during the deposition, in contrast to ordinary oblique columnar structures which are generated on the stationary substrate. Not only electric, magnetic and optical [8,9] but also chemical, medical and biological applications of thin films with hypercolumnar structures are expected [10,11].

For these applications, thin film structures should be optimized in terms of columnar shape, packing density, and surface area. A numerical simulation for thin film growth is a powerful tool to design and understand the thin-film structures from atomic [12] to mesoscopic [13, 14] scale. Recently, we developed a fully 3-dimensional (3D) Monte Carlo simulator and succeeded in reproducing hypercolumnar structures in the thin films prepared by DOD [15]. In this paper we propose a simple calibration procedure for VFIGS parameters and discuss the limits of the density modulation for the DOD thin films.

2. Growth Modeling

We designed morphologies, thickness, and density of thin films using our original fully 3D simulator, VFIGS (Virtual Film Growth System) based on the Monte Carlo ballistic deposition process [13] and surface diffusion. In this section, we describe our modeling of thin film growth briefly, since the details have been reported in [15].

The VFIGS expresses thin films as an aggregate of cubic particles which represent the statistically averaged trajectories of a large number of atoms in the thin films. A number of deposition particles are started sequentially from randomly selected positions in the plane just above the growing film surface. A particle progresses linearly in the direction determined by the geometrical deposition conditions of the deposition angle α, the dispersion of the deposition angle $\Delta\alpha$ and the azimuthal deposition direction ϕ, until at least one occupied site is found in the neighboring 26 sites.

The particle is then allowed to diffuse over the film surface. The particle diffuses by random walk depending on the local surface morphology. A new sticking particle hops to a site chosen from the neighboring 26 sites and its present position by S times. The criteria used for this choice is as following: (1) the new particle does not hop to a site occupied by another one; and (2) the hopping probability $p_{i\to j}$ from site i to allowed site j is defined as follows,

$$p_{i\to j} = \frac{\exp(\gamma N_j)}{\sum_j \exp(\gamma N_j)}, \tag{1}$$

where N_j is the coordination of the site j with its neighboring particles, γ is a constant, and the summation is taken over all allowed sites. Assuming that the energy accompanied by the new particle decreases in proportion to

the coordination of the new particle with its neighboring particles, the occupied probability of the site j in thermal equilibrium is written as Eq. (1). Physically, γ and S corresponds to the ratio of the surface energy to the temperature and the diffusion length, respectively, which may be function of many deposition conditions such as substrate temperature, source material and chamber pressure during deposition.

3. Calibration of VFIGS Parameters

The surface energy and diffusion length may be estimated by highly sophisticated experiments. However, it is not easy to estimate these parameters for surfaces with complicated morphology. Thus, the user must first calibrate γ and S parameters comparing the simulation results to experimental data. The first step of the calibration procedure was previously done by visually comparing the structure of the simulated film to the actual structure observed with a scanning electron microscope (SEM). This method is sufficient for a rough calibration and the tentative values of $\gamma \sim 0.44$ and $S = 10$ reproduced the dependence of the packing density on the deposition angle rather well for various materials [15].

Starting from these values, γ and S parameters have to be fine-tuned to accurately reproduce the experimental data for a specific material. One of the most convenient data for the calibration is so-called "tooling factor", which is the ratio of physical thickness to thickness displayed on a crystal thickness-monitor (XTM) set at a fixed position and orientation in the evaporation chamber. Measuring the tooling factor for films deposited at various α, we can find the relative change in the packing density of films. This is easier and more accurate than the measurements of the absolute packing density of films. In this work, therefore, the tooling factor is used to determine γ and S parameters that give the simulation results consistent with experiments.

The evaluation of the experimental tooling factor is straightforward. In VFIGS, on the other hand, the amount of deposition, F, is monitored by a 'virtual' XTM located at the same position as the substrate and fixed at $\alpha = 0°$, where F is defied as the thickness of the film with a packing density of 100 % deposited on the virtual XTM. Since the substrate sees a smaller effective area of the source at higher deposition angles, actual deposition rate decreases as $\cos\alpha$. As a result, the relation between F and α is as follows,

$$F = \frac{1}{\Omega} \sum_i \frac{1}{\cos\alpha_i}, \tag{2}$$

where Ω is the area of the substrate and α_i is the deposition angle when the ith particle is deposited and the summation is taken over the number of deposited particles. Thus, the simulation-tooling factor is the ratio of the thickness of the resulting film to F. Although α is varied during general DOD, it is convenient that the films for the calibration are deposited at a constant α selected between 0° and 85°. Comparing the relative changes in the experimental and simulation tooling factors, we defined γ an S parameters. Actually, the thin films are deposited at various α keeping the amount of deposition at constant, and

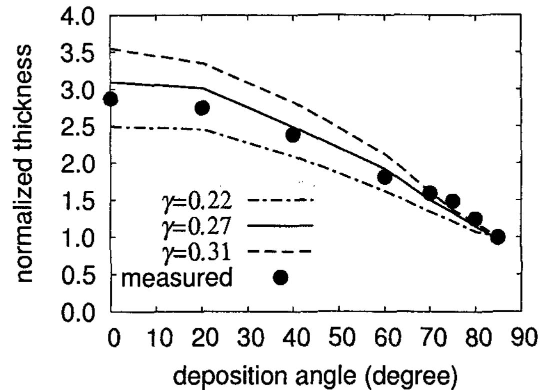

Fig. 1. The dependence of the physical thickness on the deposition angle for the films simulated using three different values of γ, where $S = 20$ and the amount of the deposition are kept constant. The thicknesses are normalized by that of the film deposited at $\alpha = 85°$. Experimental data [9] for Si films are indicated by solid circles for the comparison.

the relative change of the thickness of resulting films are compared.

4. Results and Discussion

4.1. Calibration

Recently, Kaminska *et al.* [9] tried to develop Si rugate filters using the DOD technique. They designed structure of the filters based on the relationship between α and the thickness of films which were deposited at constant α on the substrate rotated rapidly. In this work, we use their data to find the appropriate simulation parameters for Si DOD films.

Figure 1 shows the dependence of the thickness of the simulated films on α normalized by that deposited at $\alpha = 85°$. All simulation films were deposited up to $F = 158$ u on the flat substrate of 800×800 u^2, where 'u' is the unit of length in VFIGS. The lines indicate the results for the three different values of γ, while S is kept constant at 20. The data taken from [9] are also indicated by solid circles. Since the number of deposited particles depends on $\cos\alpha$ [see Eq. (2)], the thickness decreases with increasing α. However, α dependence of the physical thickness does not obey the cosine law, since the porosity increases with increasing α. As indicated in Fig. 1, α dependence of the normalized thickness is sensitive to γ. With increasing γ, the normalized thickness strongly depends on α. Since γ corresponds to the ratio of the surface energy to temperature, the deposited particles tend to aggregate (disperse) for large (small) γ. Especially at a large α, the self shadowing effect may be more effective in the case of the large γ than that of the small γ. This leads to the differences in the α dependence of the normalized thickness for the different values of γ. In comparison with the measured data, $\gamma \sim 0.27$ is appropriate for the DOD Si films.

On the other hand, the α dependence of the normalized thickness is not very sensitive to S. As we mentioned in our previous paper [15], the density of simulated thin

films gradually increased for $S \geq 10$. Thus, it is sufficient to determine the optimized γ to design the morphology of DOD films. However, S has to be calibrated in order to accurately design density related properties. For this purpose, we require data from which we can estimate the density for at least one deposition angle. The densities of the films deposited at $\alpha = 0°$ and $\gamma = 0.27$ were 0.80 and 0.92 for the values of $S = 10$ and $S = 20$, respectively, while no significant differences was found in the α dependence of the normalized thickness. Since the refractive index of the Si film deposited at $\alpha = 0°$ is close to that of bulk [9], the density should be larger than 0.9. In this work, therefore, we simulate density modulated thin films using the values of $S = 20$ and $\gamma = 0.27$. Under this condition, the unit length in VFIGS corresponds to 1.73 nm, which is reasonable for the assumption that a particle in VFIGS represents the statistically averaged trajectories of a number of atoms in the thin films. In fact, these values correctly predict not only the structures but also the optical properties of Si rugate filters as reported in our forthcoming paper [16].

4.2. Design of Density Modulated Films

By changing α during DOD, density of thin films can be controlled continuously so that properties related to the density such as refractive index, electric and thermal conductance are also modified for the purpose of practical applications. One can roughly design the depth profile of the density based on the experimental data as indicated by solid circles in Fig. 1. However, the structure of resulting films often deviates from those expected, since the surface morphology of growing DOD films is not necessarily identical with that deposited at constant α [9]. In order to design the density profile accurately, support of the growth simulation is indispensable. In this section, we present examples of thin film structures designed by VFIGS, in which the density is modulated quasi-sinusoidally.

Figure 2 indicates the cross sectional morphology of the density modulated films simulated by VFIGS. The deposition angle of ith deposited particle was set at

$$\alpha_i = A\cos\left(\frac{2\pi i}{N_p}\right) + B, \tag{3}$$

where N_p, A (fixed at 10°) and B ($50° \leq B \leq 77°$) are period, amplitude and average of the deposition angle, respectively, while the substrate was rotated rapidly. The amount of deposition was tuned as the final thickness of 10 periods film became 6.9 μm. It is easy for VFIGS to keep the thickness constant, since the appropriate amount of deposition is readily estimated by single trial deposition. By using Eq. (2), the amount of deposition and the profile of the deposition angle to prepare real films can also be estimated easily.

For all films, the columnar structure perpendicular to the substrate is clearly observed. Furthermore, periodic change in the density is also obvious for the films $B \leq 75°$. With increasing B, columns become thick, and average density decreases. While the columns gradually broaden with increasing height for the film for $B = 75°$, no significant change in the thickness of the columns is observed for the films of $B \leq 70$. In the case of $B = 77°$, only the thick columns selectively grow, and the periodic change in the density is ambiguous. For the quantitative understanding, the density profiles were calculated by taking thin slices through the simulated films, parallel to the substrate, and calculating the average density of the slices over the entire simulation area, thus obtaining the variation of the density with film thickness as shown in Fig. 3. As expected from Figs. 2(c) and (d), sinusoidal density profiles have been achieved. The average density decreases from 0.77 to 0.37 depending on B. On the other hand, the amplitude of the density increases from 0.04 to 0.11 with increasing B. For the films deposited at $B \geq 75°$, however, the amplitude of the density decreases with increasing the films thickness. This degradation of the density oscillation is closely related to the broadening of columns as seen in Fig. 2, and is not due to a result of heating of the substrate but intrinsic to the

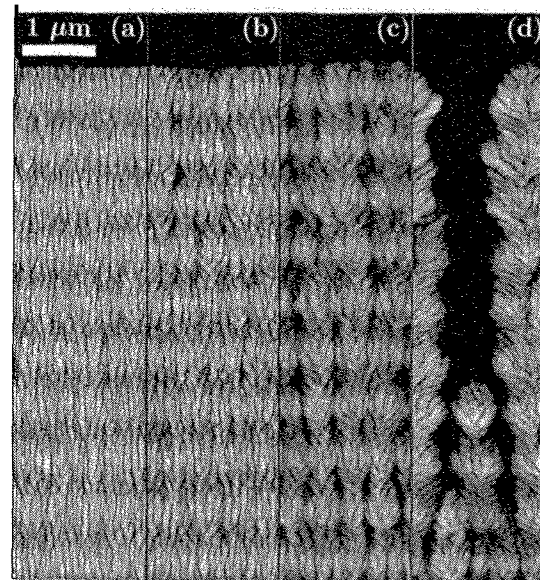

Fig. 2. Cross sectional morphology of simulated density modulated thin films of (a) $B = 60°$, (b) $B = 70°$, (c) $B = 75°$ and (d) $B = 77°$.

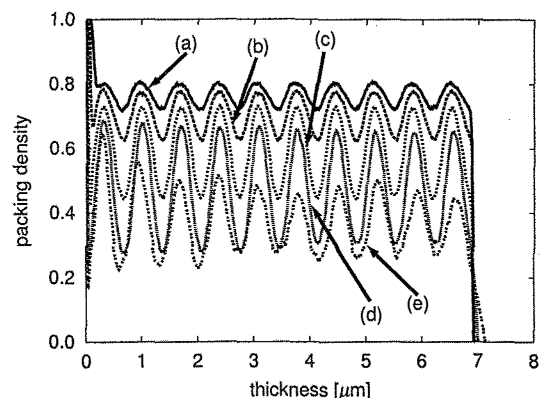

Fig. 3. Evolution of in-plane density of simulated films of (a) $B = 50°$, (b) $B = 60°$, (c) $B = 70°$, (d) $B = 75°$ and (e) $B = 77°$.

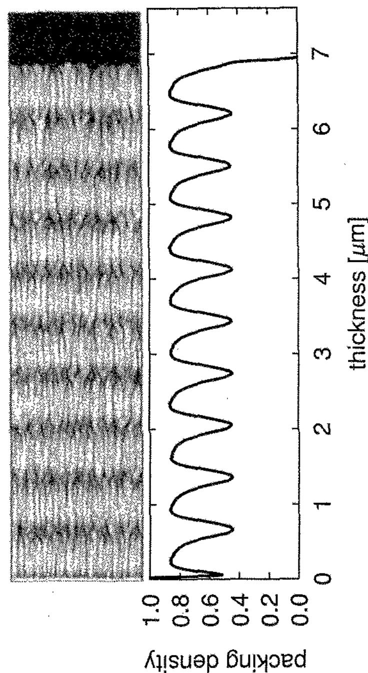

Fig. 4. Cross sectional morphology and the evolution of the packing density of the simulated film of $A = 40°$ and $B = 40°$.

growth process of DOD films. Our detailed investigation for various combinations of A and B suggests that the degradation becomes remarkable when the maximum α exceeds 85°. Therefore, α should be kept smaller than 85° in order to accurately control the thin film morphology as well as properties.

Under this limitation, we demonstrated the maximum modulation of the density by setting $A = 40°$ and $B = 40°$ ($0° \leq \alpha \leq 80°$). Figure 4 indicates the cross sectional morphology of thus simulated thin film together with the evolution of the density. The amount of deposition is also tuned as the total thickness becomes 6.9 μm. The columnar structure with a periodic change of the porosity grows into the direction perpendicular to the surface without significant broadening. Although A is four times larger than that for the films shown in Fig. 2, the packing density changes with almost constant amplitude and period. Maximum and minimum density in the density profile except for the very early stage is 0.86 and 0.45, respectively. It is remarkable that such large modulation of the density is produced by a simple deposition process. Provided that the film is made of Si, the refractive index is expected to vary from 1.6 to 2.8 by an estimation based on Lorentz–Lorenz theory. One can deign the optical filters with continuous and arbitrary refractive index profile in which the difference in the refractive index is larger than 1. Such filters will be useful for the applications to the optical communication and its related devices. The experimental verification will be presented in our forthcoming paper [16].

5. CONCLUSION

In order to design not only the morphology but also the density profile of the DOD thin films, we have successfully calibrated the parameters of fully 3D thin film growth simulator VFIGS. Using the parameters calibrated for Si by the simple procedure, we simulated the density modulated thin films which were deposited by varying the deposition angle sinusoidally. When the maximum α exceeds 85°, significant columnar broadening has occurred, and the amplitude of the density oscillation has been degraded. On the other hand, the amplitude and the period of the density are kept constant when the maximum α is less than 85°. The density can be controlled arbitrarily between 0.45 and 0.86 which corresponds to the refractive index variation between 1.6 and 2.8 for Si. The precisely controlled density modulated thin films are applicable for wide variety of optical rugate filters.

6. ACKNOWLEDGMENT

This work was supported by The 21st Century COE Program "Center of Excellence for Research and Education on Complex Functional Mechanical Systems" and by The Mazda Foundation's Research Grant.

REFERENCES

1. R. Messier, A. Lakhtakia, Mat. Res. Innovat. **2**, 217–222 (1999).
2. H. van Kranenburg, C. Lodder, Mat. Sci. Eng. **R11**, 295–354 (1994).
3. T. Motohiro, Y. Taga, Appl. Opt. **28**, 2466–2482 (1989).
4. M. Suzuki, T. Ito, Y. Taga, Proc. SPIE **3790**, 94–105 (1999).
5. K. Robbie, M. J. Brett, A. Lakhtakia, J. Vac. Sci. Technol. A **13**, 2991–2993 (1995).
6. K. Robbie, L. J. Friedrich, S. K. Dew, T. Smy, M. J. Brett, J. Vac. Sci. Technol. A **13**, 1032–1035 (1995).
7. M. Suzuki, Y. Taga, Jpn. J. Appl. Phys. Part 2 **40**, L358–L359 (2001).
8. R. M. A. Azzam, Appl. Phys. Lett. **61**, 3118–3120 (1992).
9. K. Kaminska, T. Brown, G. Beydaghyan, K. Robbie, App. Opt. **42**, 4212–4219 (2003).
10. A. Lakhtakia, R. Messier, M. J. Brett, K. Robbie, Innov. Mater. Res. **1**, 165–176 (1996).
11. M. Suzuki, T. Ito, Y. Taga, Phys. Lett. **78**, 3968–3970 (2001).
12. H. Huang, G. H. Gilmer, T. D. de la Rubia, J. Appl. Phys. **84**, 3636 (1998).
13. P. Meakin, P. Ramanlal, L. M. Sander, R. C. Ball, Phys. Rev. A **34**, 5091 (1986).
14. T. Smy, D. Vick, M. J. Brett, S. K. Dew, A. T. Wu, J. C. Sit, K. D. Harris, J. Vac. Sci. Technol. A **18**, 2507–2512 (2000).
15. M. Suzuki, Y. Taga, J. Appl. Phys. **90**, 5599–5605 (2001).
16. K. Kaminska, M. Suzuki, K. Kimura, Y. Taga, K. Robbie (to be published).

(Received October 10, 2003; Accepted March 31, 2004)